Electromagnetic Ion Cyclotron Waves in the Initial Phase of Geomagnetic Storms

Taylor Whitney Aegerter[1,2] (`Taylor.WhitneyAegerter@colorado.edu`) **& Lauren Blum**[1,2]

[1]University of Colorado Boulder, Department of Astrophysical and Planetary Sciences, Boulder CO, United States
[2]Laboratory for Atmospheric and Space Physics, Boulder CO, United States

Whitney Aegerter, T. R. and Blum, L. W. (2026). Electromagnetic Ion Cyclotron Waves in the Initial Phase of Geomagnetic Storms. *Geophysical Research Letters*. [under review]

Motivation

- In a collisionless magnetosphere, plasma waves are the primary mechanism for energy and momentum transfers across particle populations [4, 11]
- EMIC waves lead to losses of ring current ions and of radiation belt electrons as well as heating of cold electrons [e.g. 1, 16]
- Overlapping spacecraft missions in Earth's inner magnetosphere enable assessment of instantaneous regions of EMIC activity
- **Science Question:** Where and how are inner magnetosphere EMIC waves generated in response to initial compressions by geomagnetic storms?

Methods

- Combined satellite magnetic field observations
  - 10 satellites from Van Allen Probes, MMS, THEMIS, and GOES
  - September 2015 - October 2019
  - 79 geomagnetic storms, 23 with well-defined initial phases (adapted from the Pedersen et al. (2024) list [7])
- EMIC wave detection algorithm
  - Similar to Bortnik et al. (2007) [3]
  - Only events inside the magnetopause (modeled by Shue et al. (1998) [9])
  - Manual adjustments to rule out false detections
- EMIC detections and regions of activity to determine spatial distribution
- Comparison of EMIC detections to time elapsed in initial phase and storm parameters to determine differences between dayside and nightside activity

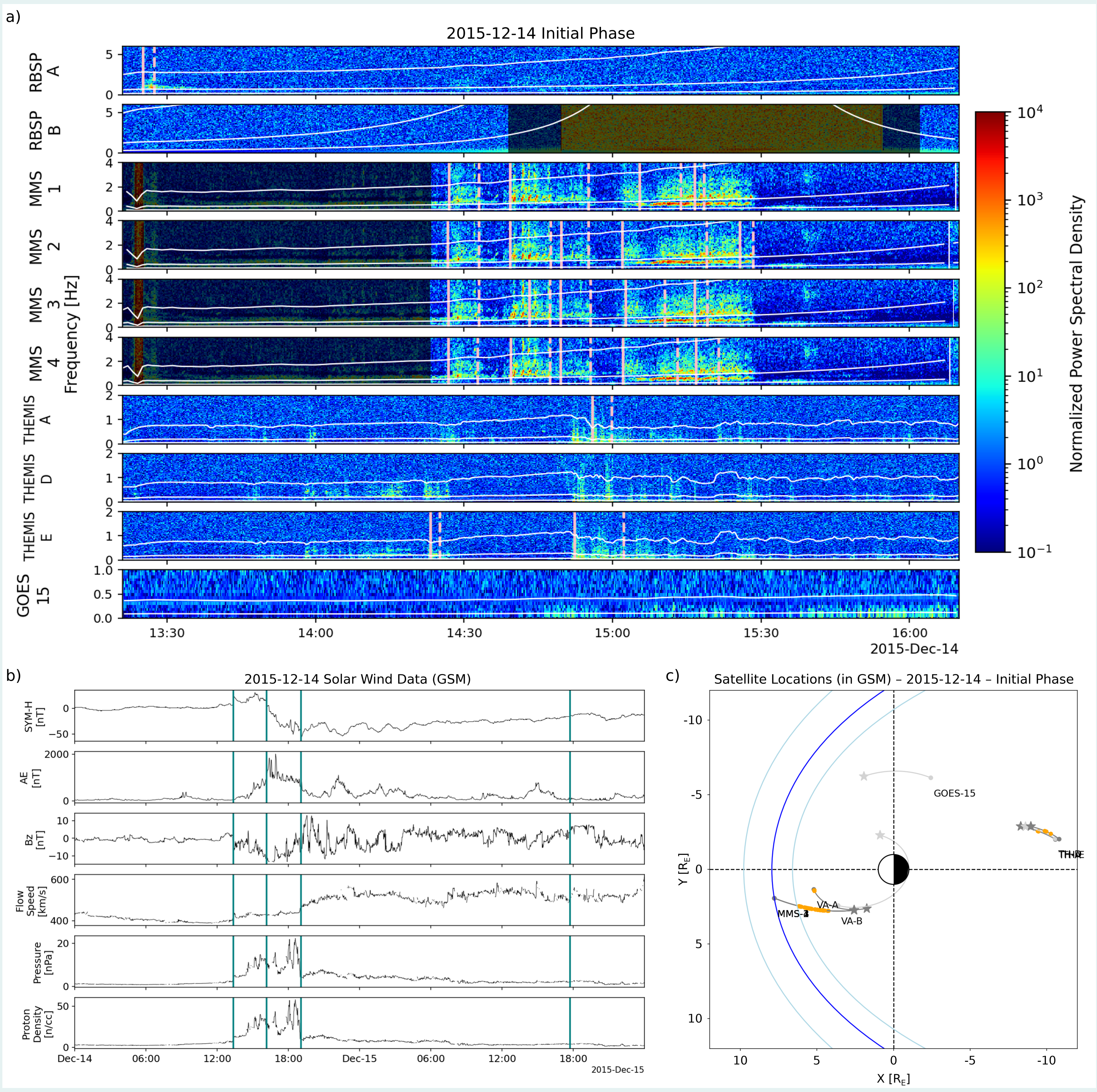

Figure: EMIC detection process for the initial phase on December 14, 2015 including a) spectrograms from all 10 spacecraft with EMIC wave start (solid) and end (dashed) times in pink, b) solar wind and geomagnetic parameters for the entire storm, and c) EMIC detections along satellite orbits

Background

- EMIC waves are generated in the Earth's inner magnetosphere by anisotropic ion distributions with energies of approximately 1 - 100 keV and can be measured in the range from 0.1 - 5 Hz [5, 12, 16]
- Waves are often more prevalent during increased geomagnetic activity [10] with occurrence rates up to 10% [e.g. 6, 8, 14]
  - When present, an initial phase compresses the dayside of the magnetosphere and can increase the geomagnetic field strength to trigger ion temperature anisotropy and wave generation there [2, 10, 13, 14, 16, 15]
  - In the main and recovery phases, temperature anisotropy can adiabatically develop when ions injected from the magnetotail are convected into the inner magnetosphere [12]

Distribution of EMIC Waves

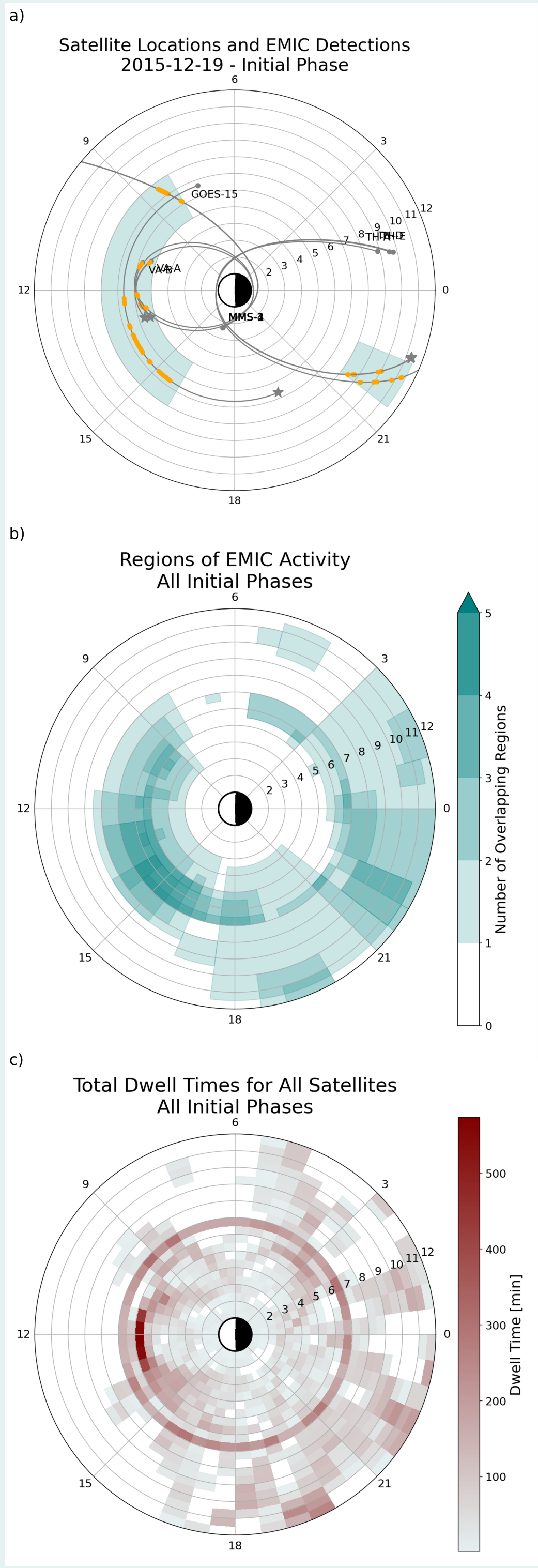

Figure: Spatial distribution of EMIC waves including a) individual regions of activity for the December 19, 2015 initial phase, b) regions of activity for all 23 initial phases, and c) dwell time (minutes) for all observations inside the magnetopause

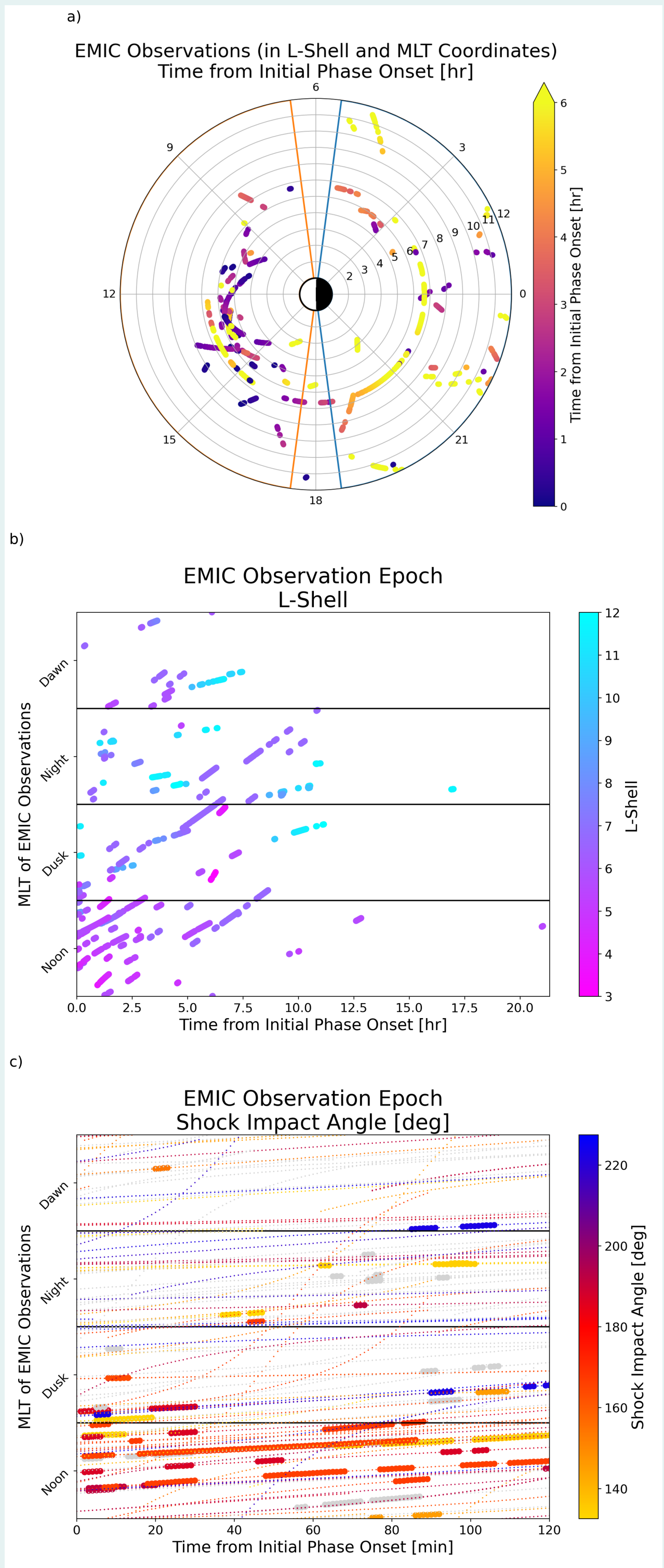

Figure: Temporal distribution of EMIC waves including a) all EMIC detections in L-MLT coordinates colored by elapsed time, b) all EMIC detections in elapsed time vs MLT colored by L-shell, and c) EMIC detections in the first 120 minutes of storms colored by shock impact angle

Conclusions

- Over 50% of initial phases had EMIC activity on the nightside, contrary to our hypothesis.
- Dayside activity dominates the beginning of an initial phase, as expected. There is a lag of at least 35 minutes before nightside EMIC waves begin.

Acknowledgments

This work was funded by the NSF AGS grant 2442556 as well as the Air Force Institute of Technology. The views, opinions, and/or findings expressed are those of the authors and should not be interpreted as representing the official views or policies of the Department of Defense or the U.S. Government. The authors would also like to thank the scientists, engineers, and team members of the many missions utilized in this study, including but not limited to Van Allen Probes, MMS, THEMIS, GOES, and the PySPEDAS Python package.

Solar Wind and Geomagnetic Drivers

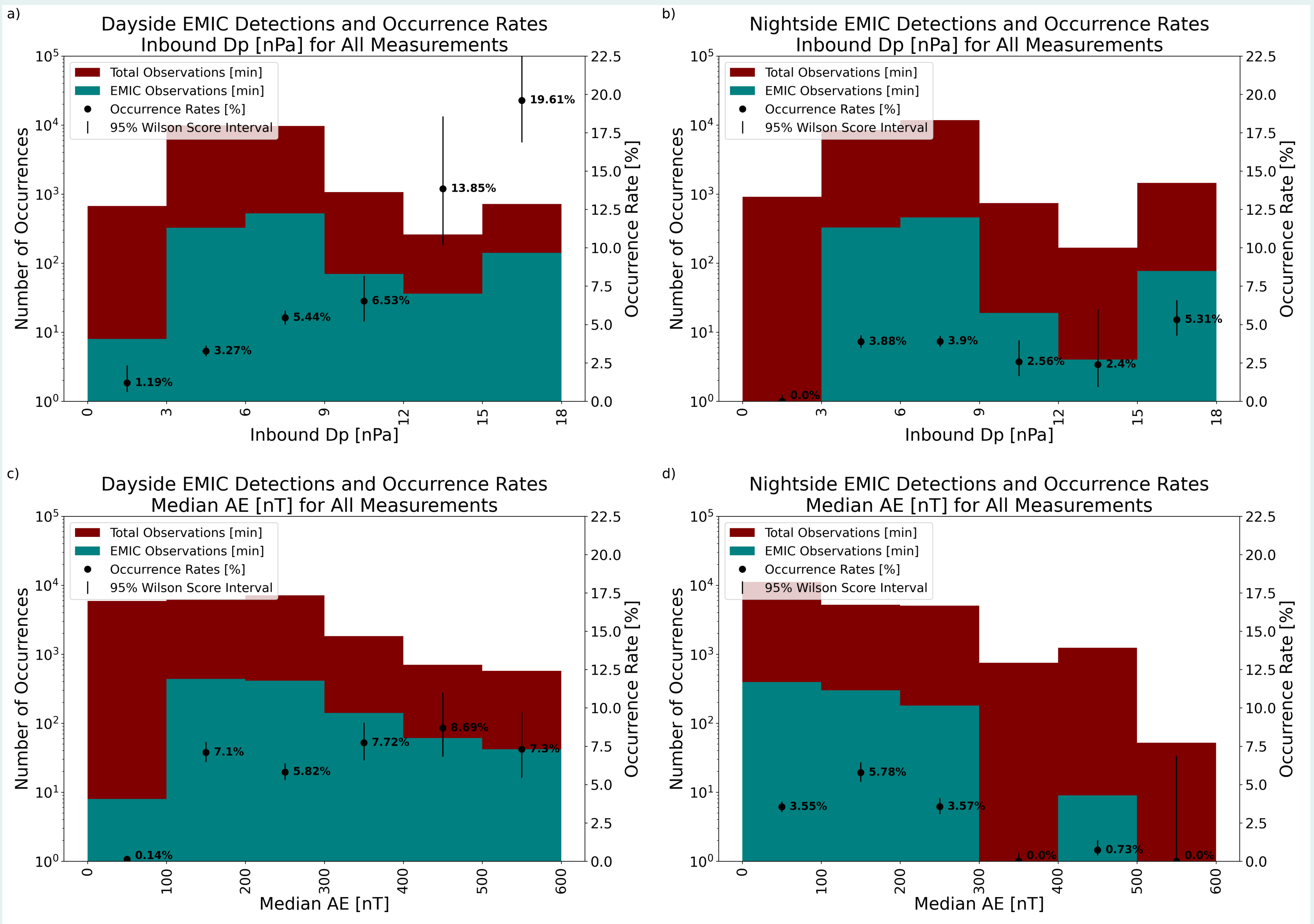

Figure: Comparison of solar wind dynamic pressure and AE index in dayside vs nightside EMIC activity with all observations in red, EMIC observations in teal, and occurrence rates in black with error bars of Wilson score intervals with a 95% significance level

Conclusions

- Differences between dayside and nightside waves can be seen in the shock impact angle, inbound solar wind pressure, and median AE index value.
  - Frontal shocks drive dayside EMIC activity while oblique shocks are more often associated with nightside EMIC activity.
  - Dayside EMIC activity occurrence rates increase with inbound solar wind pressure. In the nightside magnetosphere, once a threshold is met (> 3 nPa), there is a similar likelihood that EMIC activity will occur regardless of the inbound solar wind pressure.
  - Dayside EMIC occurrence rates increase with increasing substorm activity while nightside occurrence rates are lowest for the highest AE levels.

References

[1] L. W. Blum et al. (2019). DOI: `10.1029/2018JA026427`.
[2] L. W. Blum et al. (2021). DOI: `10.1029/2021GL092700`.
[3] J. Bortnik et al. (2007). DOI: `10.1029/2006JA011900`.
[4] D. A. Gurnett (1985). DOI: `10.1029/GM035p0207`.
[5] K. Keika et al. (2013). DOI: `10.1002/jgra.50371`.
[6] K. Keika et al. (2013). DOI: `10.1002/jgra.50385`.
[7] M. N. Pedersen et al. (2024). DOI: `10.1029/2024JA032656`.
[8] A. A. Saikin et al. (2016). DOI: `10.1002/2016JA022523`.
[9] J.-H. Shue et al. (1998). DOI: `10.1029/98JA01103`.
[10] R. M. Thorne et al. (2021). DOI: `10.1002/9781119815624.ch6`.
[11] R. M. Thorne (2010). DOI: `10.1029/2010GL044990`.
[12] M. E. Usanova et al. (2016). DOI: `10.1002/9781119055006.ch5`.
[13] M. E. Usanova et al. (2008). DOI: `10.1029/2008GL034458`.
[14] M. E. Usanova et al. (2012). DOI: `10.1029/2012JA018049`.
[15] Z. Xue et al. (2022). DOI: `10.1029/2022GL098954`.
[16] Z. Xue et al. (2021). DOI: `10.1029/2020GL091479`.